11-1-1995

A Magnetic, Neutron-diffraction, and Mössbauer Spectral Study of the $Ce_2Fe_{17-x}Si_x$ Solid Solutions

D. P. Middleton

Sanjay R. Mishra

Gary J. Long
Missouri University of Science and Technology, glong@mst.edu

Oran Allan Pringle
Missouri University of Science and Technology, pringle@mst.edu

et. al. For a complete list of authors, see http://scholarsmine.mst.edu/chem_facwork/775

Recommended Citation

D. P. Middleton et al., "A Magnetic, Neutron-diffraction, and Mössbauer Spectral Study of the $Ce_2Fe_{17-x}Si_x$ Solid Solutions," *Journal of Applied Physics*, vol. 78, no. 9, pp. 5568-5576, American Institute of Physics (AIP), Nov 1995.
The definitive version is available at http://dx.doi.org/10.1063/1.359678

A magnetic, neutron-diffraction, and Mössbauer spectral study of the $Ce_2Fe_{17-x}Si_x$ solid solutions

D. P. Middleton
Philips Research Laboratories, NL-5656 AA Eindhoven, The Netherlands

S. R. Mishra, Gary J. Long, and O. A. Pringle
Departments of Physics and Chemistry, University of Missouri-Rolla, Rolla, Missouri 65401-0249

Z. Hu and W. B. Yelon
University of Missouri Research Reactor and the Departments of Chemistry and Physics, University of Missouri-Columbia, Columbia, Missouri 65211

F. Grandjean
Institute of Physics, B5, University of Liège, B-4000 Sart-Tilman, Belgium

K. H. J. Buschow
Van der Waals–Zeeman Laboratory, University of Amsterdam, NL-1018 XE Amsterdam, The Netherlands

(Received 24 April 1995; accepted for publication 8 July 1995)

The magnetic properties of a series of $Ce_2Fe_{17-x}Si_x$ solid solutions with x equal to 0.0, 0.23, 0.4, 0.6, 0.8, 1.02, 1.98, and 3.20 have been studied by magnetic measurements, neutron diffraction, and Mössbauer spectroscopy. An x-ray-diffraction study indicates that the compounds adopt the rhombohedral Th_2Zn_{17}-type structure. The substitution of silicon for iron in Ce_2Fe_{17} leads to a contraction of the a axis by 0.2%, an expansion of the c axis by 0.2%, and a consequent reduction of the unit-cell volume by about 0.2% per substituted silicon. Magnetization studies indicate that the Curie temperature increases uniformly from 238 K for Ce_2Fe_{17} to 455 K for $Ce_2Fe_{14}Si_2$. Powder neutron-diffraction results, obtained at 295 K, indicate both that the silicon atoms preferentially occupy the 18h sites and that the iron moments increase with increasing silicon content, an increase which is related to the increase in Curie temperature. The Mössbauer spectra have been fit with a binomial distribution of the near-neighbor environments in terms of a maximum hyperfine field H_{max} for an iron with zero silicon near neighbors, and a decremental field ΔH per silicon near neighbor. The compositional independence of both the weighted average maximum hyperfine field and of the decremental field indicates that the silicon acts as a magnetic hole, a hole which does not perturb the magnetic moments at the iron sites. The compositional dependence of the weighted average isomer shift is explained in terms of an interband mixing of the iron 4s and silicon 2p bands, due to the reduction of the iron 18h bond lengths. This interband mixing affects the charge but not the spin distribution at the iron sites. © *1995 American Institute of Physics.*

I. INTRODUCTION

Intermetallic compounds suitable for permanent magnet applications require high magnetizations, high coercivities, and high Curie temperatures. Powerful permanent magnet materials are based on compounds such as $SmCo_5$ and $Nd_2Fe_{14}B$. The $SmCo_5$-based materials are expensive due to the high cost and limited availability of the raw materials. Iron-rich compounds are less expensive but have rather low Curie temperatures. The discovery of the ternary $Nd_2Fe_{14}B$ compound has led to a revival of the search for novel rare-earth (R) 3d transition-metal compounds which have favorable magnetic properties due both to the rare-earth sublattice and the 3d sublattice. The rare-earth sublattice is the main contributor to the magnetocrystalline anisotropy at room temperature, whereas the 3d sublattice is mainly responsible for the sufficiently high magnetic ordering temperatures.

The discovery by Coey *et al.*[1] that interstitial compounds of the type $R_2Fe_{17}N_x$ have increased Curie temperatures has led to numerous studies of the R_2Fe_{17} materials for permanent magnet applications. The Curie temperatures of the $R_2Fe_{17}N_x$ compounds are significantly higher than those of the $Nd_2Fe_{14}B$ compounds, but are still lower than that of $SmCo_5$. Moreover, among all the $R_2Fe_{17}N_x$ compounds only $Sm_2Fe_{17}N_x$ exhibits uniaxial anisotropy. Therefore, it is important to search for other modifications of R_2Fe_{17} compounds, through partial substitution of iron by atoms such as silicon, aluminum, or gallium, which may lead to even higher Curie temperatures and perhaps to a change from planar to uniaxial anisotropy.

Recent investigations[2] of $Tb_2Fe_{17-x}Ga_x$ show that partial substitution of gallium for iron leads to increases in the Curie temperature of ~150 K above that of Tb_2Fe_{17}. The Curie temperature reaches a maximum between $Tb_2Fe_{14}Ga_3$ and $Tb_2Fe_{13}Ga_4$, and decreases with further increases in x. Magnetic powder neutron-diffraction results indicate[2] that there is a change in easy magnetization direction from planar to axial with increasing gallium concentration. As in the case of nitrogenation to form $R_2Fe_{17}N_x$, gallium substitution also leads to an increase in the unit-cell volume. Previous investigations[3] of the combined effect of substitutional aluminum and interstitial nitrogen in Ce_2Fe_{17} have shown an increase in the unit-cell volume and an increase in the Curie temperature by ~480 K.

 0021-8979/95/78(9)/5568/9/$6.00

At low concentrations, silicon substitution increases the Curie temperature and reduces the unit-cell volume of the $R_2Fe_{14}B$ compounds[4–6] with a minor concurrent reduction of the saturation magnetization and coercivity. Previous investigations have also shown[7–11] that the replacement of iron in the R_2Fe_{17} compounds by diamagnetic silicon leads to an increase in their Curie temperatures, an increase which is accompanied by a reduction in the unit-cell volumes with increasing silicon content. Recently we have reported,[12] based on a neutron-diffraction and Mössbauer effect study of the $Nd_2Fe_{17-x}Si_x$ compounds, that silicon preferentially occupies the $18h$ site in the Nd_2Fe_{17} structure. Silicon substitution leads to a contraction of the lattice except around the $18h$ site, which, along with the $9d$ site, expands the most upon substitution. To date, there has been no thorough explanation of the increases in the Curie temperatures of these silicon-substituted compounds. Earlier, we attributed[12] the increases in Curie temperatures to the expansion of the lattice in the $9d-18h$ plane of the unit cell of the $Nd_2Fe_{17-x}Si_x$ solid solutions. Recently, Woods *et al.*[13] have calculated the Curie temperatures of several iron-based rare-earth permanent magnet compounds by using self-consistent spin-polarized electronic structure calculations and the spin-fluctuation theory of Mohn and Wohlfarth. They also measured changes in the density of states at the Fermi level for interstitial and substitutional modifications by means of soft-x-ray photoemission experiments and found that the changes compared well with their[13] calculations. However, an explanation of the Curie temperature increase in the silicon substituted compounds is still lacking. In this article we report the results of a magnetic, neutron-diffraction, and Mössbauer spectral study of the $Ce_2Fe_{17-x}Si_x$ solid solutions.

II. EXPERIMENTAL METHODS

The samples were prepared from 99.9% pure elements by arc melting in an argon atmosphere. After arc melting, the samples were wrapped in tantalum foil and were vacuum annealed in quartz tubes at 900 °C for 2 weeks. The samples were investigated by powder x-ray diffraction with Cu $K\alpha$ radiation on a Philips PW 1800/10 x-ray diffractometer equipped with a single-crystal monochromator. The magnetic measurements were performed on field-cooled free particle samples at Philips Research Laboratories, on a superconducting quantum interference device (SQUID) magnetometer for temperatures between 5 and 350 K and on a Faraday magnetometer for temperatures between 350 and 1000 K. The Curie temperatures were determined in small magnetic fields of 0.1 T by plotting the magnetization versus temperature and extrapolating the steepest part of the curve to zero magnetization. Values of the saturation magnetization at 5 K were obtained from the magnetic isotherms by extrapolating the $M(1/B)$ curves to $1/B=0$.

The powder neutron-diffraction patterns were collected at the University of Missouri Research Reactor by using a linear position sensitive detector and neutrons with a wavelength of 1.4783 Å. The data for each sample were collected at 295 K between 2θ angles of 5° and 105° on approximately 2 g of finely powdered sample placed in a thin wall vanadium container. Refinements of the neutron-diffraction data

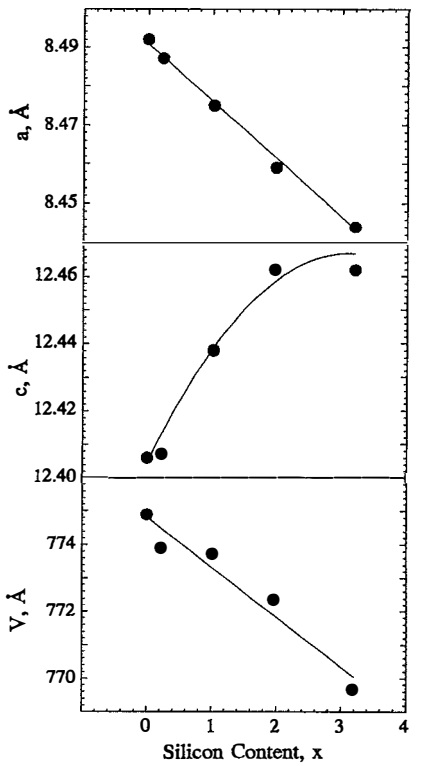

FIG. 1. The concentration dependence of the a and c lattice parameters and the unit-cell volume of $Ce_2Fe_{17-x}Si_x$ derived from 295 K powder neutron-diffraction results.

were carried out with the FULLPROF computer code[14] which permits multiple phase refinement as well as magnetic structure refinement of each of the coexisting phases. The $Ce_2Fe_{17-x}Si_x$ solid solutions were found to contain at most ~7% of α-iron.

The Mössbauer spectra were obtained at the University of Missouri-Rolla on a constant-acceleration spectrometer which utilized a room-temperature rhodium matrix cobalt-57 source and was calibrated at room temperature with α-iron foil. The Mössbauer absorbers, which were ~30 mg/cm^2, were prepared from powdered samples which had been sieved to a 0.045 mm or smaller particle diameter. The resulting spectra have been fit as discussed below and elsewhere[15] and the estimated errors are ±2 kOe for the weighted average maximum hyperfine fields H_{max} and the incremental fields ΔH, and ±0.01 mm/s for the weighted average isomer shifts δ. The hyperfine parameters for the α-iron phase were constrained to their known values.

III. RESULTS

The x-ray and powder neutron-diffraction patterns indicate that the $Ce_2Fe_{17-x}Si_x$ solid solution lattice parameters change with increasing silicon content. The effect of silicon substitution on the crystallographic properties of Ce_2Fe_{17}, is very similar to the effect of silicon substitution in Nd_2Fe_{17}. As is shown in Fig. 1 for the neutron-diffraction results, the a axis decreases linearly by ~0.2% per substituted silicon, whereas the c axis increases by ~0.2% per substituted sili-

TABLE I. The 295 K x-ray crystallographic parameters, the 4.2 K magnetic properties, and the mean-field theory derived exchange coupling constant for $Ce_2Fe_{17-x}Si_x$.

Nominal Si content x	a axis (Å)	c axis (Å)	μ_S/fu. (μ_B)	μ_{Fe} (μ_B)	J_{FeFe}/k_B (K)
0[a]	8.491	12.409	32.80	1.93	19
0.2	8.486	12.412	31.60	1.88	...
0.4	8.484	12.408	...	...	...
0.6	8.478	12.420	...	...	...
0.8	8.477	12.429	...	...	...
1.0	8.456	12.472	29.01	1.81	31
2.0	8.457	12.428	27.36	1.82	42
3.0	8.441	12.424	23.56	1.68	54

[a]Obtained from Ref. 23.

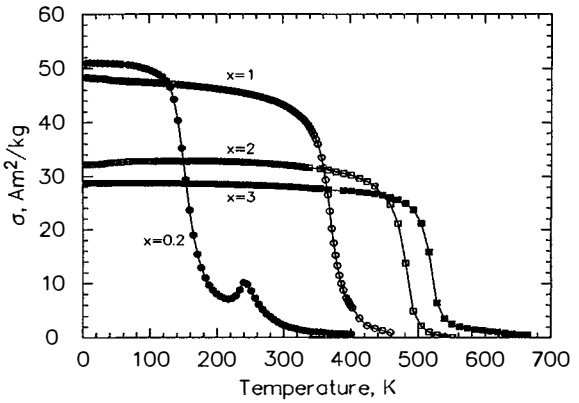

FIG. 2. The temperature dependence of the magnetization $\sigma(T)$ of $Ce_2Fe_{17-x}Si_x$, measured at 0.1 T for field-cooled free particle samples.

con. These changes give rise to an approximately linear decrease in the unit cell volume of ~0.2% per substituted silicon, as is shown in Fig. 1. Numerical values for these parameters are given in Tables I and II.

The magnetization of the $Ce_2Fe_{17-x}Si_x$ solid solutions was measured as a function of temperature in a 0.1 T field. As is shown in Fig. 2, the magnetization of $Ce_2Fe_{16.8}Si_{0.2}$ shows a cusplike anomaly at 210 K an anomaly which we associate with a transition to helimagnetically ordered iron moments below this temperature. This type of transition has been reported[16,17] to occur in Ce_2Fe_{17} at a temperature between 4.2 and 140 K.

As noted in Sec. II, the temperature dependence of the magnetization has been used to determine the Curie temperatures of the $Ce_2Fe_{17-x}Si_x$ solid solutions. The resulting compositional dependence of the Curie temperature is shown in Fig. 3. The Curie temperature increases with x and tends to saturate as the silicon solubility limit[18] is reached at $Ce_2Fe_{14}Si_3$. Apparently the substitution of silicon for iron leads to the disappearance of the fan-magnetic arrangement of the iron moments found[16] in Ce_2Fe_{17} at 5.0 K. In the presence of the substitutional silicon, ferromagnetism prevails and results in the disappearance of the metamagnetic transition, a transition which is apparent in Fig. 4 for Ce_2Fe_{17} at low $\mu_0 H$ values. From a comparison[5,19] of the saturation magnetizations of $Ce_2Fe_{17-x}Si_x$ and $Y_2Fe_{17-x}Si_x$ and by taking into account the induced antiparallel yttrium moment[20] of ~$0.2\mu_B$, one can infer that cerium is in either a tetravalent or a mixed valent state.[21,22] The magnetic isotherms measured at 5 K, shown in Fig. 4, yield values of the saturation magnetization per formula unit and the concomitant iron magnetic moments given in Table I.

TABLE II. The lattice and positional parameters, site occupancies, and moments in $Ce_2Fe_{17-x}Si_x$ as measured by neutron diffraction at 295 K.

Compound	Ce_2Fe_{17}	$Ce_2Fe_{16.8}Si_{0.2}$	$Ce_2Fe_{16}Si$	$Ce_2Fe_{15}Si_2$	$Ce_2Fe_{14}Si_3$
x refined	0.00	0.23	1.02	1.98	3.20
a, Å	8.4921(2)	8.4870(2)	8.4753(2)	8.4596(2)	8.4449(3)
c, Å	12.4060(3)	12.4071(2)	12.4380(3)	12.4620(4)	12.4618(4)
c/a	1.4608	1.4618	1.4675	1.4731	1.4757
V, Å^3	774.81(6)	773.94(5)	773.73(6)	772.36(6)	769.66(8)
Ce, 6c, z	0.3441(5)	0.3441(6)	0.3426(6)	0.3419(6)	0.3405(7)
Fe/Si, 6c, z	0.0970(2)	0.0969(3)	0.0966(3)	0.0963(2)	0.0960(3)
Fe/Si, 18f, x	0.2905(1)	0.2908(2)	0.2932(2)	0.2952(2)	0.2966(2)
Fe/Si, 18h, x	0.1678(1)	0.1678(1)	0.1677(2)	0.1676(1)	0.1673(2)
Fe/Si, 18h, z	0.4883(1)	0.4882(2)	0.4890(3)	0.4899(2)	0.4906(2)
% Si, 6c	0.0	0.0	0.0	0.0	0.0
% Si, 9d	0.0	0.0	1.2	4.8	10.4
% Si, 18f	0.0	0.0	0.0	2.0	8.4
% Si, 18h	0.0	3.8	16.6	28.6	39.8
R factor	5.05	6.13	6.03	6.11	6.65
R_w factor	7.11	8.13	8.51	8.69	9.29
R_m factor	...	...	7.53	7.66	10.60
χ^2	2.91	3.31	4.56	4.58	4.93
μ_{Fe}, 6c, μ_B	...	...	0.38	1.0(2)	2.0(3)
μ_{Fe}, 9d, μ_B	...	...	0.38	1.0(2)	1.6(3)
μ_{Fe}, 18f, μ_B	...	...	0.38	1.0(2)	1.9(2)
μ_{Fe}, 18h, μ_B	...	...	0.38	1.0(2)	1.3(2)
α-Fe, vol %	5.6	7.56	1.96	7.66	3.88

The exchange coupling constant J_{FeFe} has been calculated by means of a mean-field analysis of the Curie temperature T_C. The mean-field analysis gives

$$T_C = 2J_{FeFe}Z_{FeFe}G_{Fe}/3k_B, \tag{1}$$

where

$$Z_{FeFe} = 10\left(1 - \frac{x}{17}\right), \tag{2a}$$

$$G_{Fe} = S_{Fe}(S_{Fe}+1), \tag{2b}$$

$$S_{Fe} = \frac{\mu_{Fe}}{2\mu_B}, \tag{3}$$

and Z_{FeFe} is the number of nearest iron neighbor atoms. As is indicated by Eq. (1), J_{FeFe} can be determined from the experimental values[23] of T_C and μ_{Fe} listed in Table I, which also gives the resulting values of J_{FeFe}.

The results of the refinement of the 295 K powder neutron-diffraction patterns of the $Ce_2Fe_{17-x}Si_x$ samples are given in Table II. The neutron diffraction derived unit-cell parameters for the $Ce_2Fe_{17-x}Si_x$ solid solutions agree very well with those obtained by x-ray powder diffraction and given in Table I. As is shown in Fig. 5, silicon preferentially occupies the $18h$ site in the Ce_2Fe_{17} structure, the site with the largest number of near-neighbor cerium atoms. Silicon also shows a minor preference for the $9d$ and $18f$ sites for $x \geq 1$. Silicon completely avoids the $6c$ or dumbbell site for all x values and this site remains completely occupied by iron. The refinement assumes both a stoichiometric occupation of the transition-metal sites and a basal plane alignment of the iron magnetic moments. At $x=0.0$ and 0.23 silicon content, the compounds are paramagnetic at 295 K. Because the magnetic scattering is weak, it is not possible to independently refine the magnetic moments on the different iron sites for $x=1$ and 2, but the average iron moments tend to increase with increasing silicon content at 295 K. For $Ce_2Fe_{13.8}Si_{3.2}$ it was possible to refine different moments on the different iron sites and, as expected, the $6c$ site has the largest and the $18h$ site the lowest moment. For this compound, the average magnetic moment calculated from these individual iron site moments agrees exactly with the average saturation iron moment given in Table I. The overall increase in the moments with x is most likely associated with the increase in Curie temperature and the concomitant larger degree of magnetic order present at room temperature.

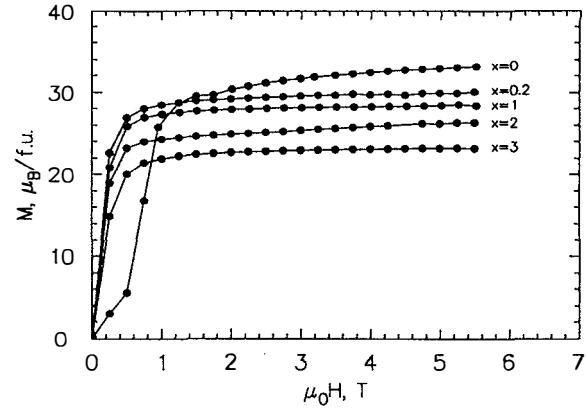

FIG. 4. The magnetic isotherms of the $Ce_2Fe_{17-x}Si_x$ solid solutions measured at 5.0 K.

The Mössbauer spectra can reveal details of the effect of silicon substitution on the electronic properties of $Ce_2Fe_{17-x}Si_x$. The Mössbauer spectra reported herein have been fit with a model in which the magnetization and hyperfine field lie in the basal plane of the unit cell. Under the combined effect of the dipolar field and quadrupole interaction, the Mössbauer spectra of $Ce_2Fe_{17-x}Si_x$ are composed of seven magnetic components representing the $6c$, $9d_6$, $9d_3$, $18f_{12}$, $18f_6$, $18h_{12}$, and $18h_6$ magnetically inequivalent iron sites. The difference in the hyperfine fields of the crystallographically equivalent, but magnetically inequivalent, sites results from the dipolar field arising from the iron $3d$ spin moment and the orbital field due to $3d$ orbital moments.[24] Because the near-neighbor environment of a particular iron site is influenced by the presence of silicon, a distribution of the hyperfine parameters results at each iron site. By using the silicon occupancy obtained from the neutron-diffraction results listed in Table II, the binomial distribution of the silicon near neighbors of a specific iron site can be calculated. Thus, in the Mössbauer spectral fits, the

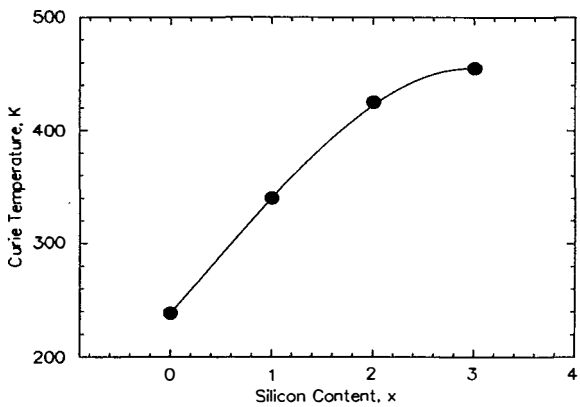

FIG. 3. The Curie temperature of $Ce_2Fe_{17-x}Si_x$ as a function of the silicon content x.

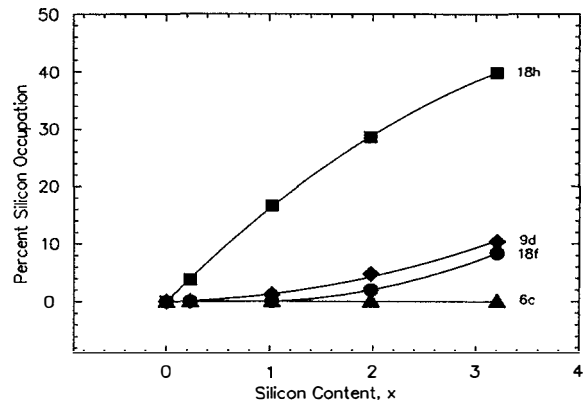

FIG. 5. The percentage of silicon on the four crystallographic iron sites in $Ce_2Fe_{17-x}Si_x$, as a function of silicon content.

sextet corresponding to a given crystallographically and magnetically unique iron site is replaced by several sextets, each resulting from an iron atom on the site having a different number of silicon near neighbors. The hyperfine field $H(x,n)$ at a given iron site, with n silicon near neighbors, is then given by $H(x,n)=H_{\max}-n\Delta H(x)$, where $H_{\max}$ is the hyperfine field at an iron site which has zero silicon near-neighbor atoms, and the decremental field ΔH is the decrease in the hyperfine field when one near-neighbor iron is replaced by silicon. In all cases the distribution of quadrupole interactions and of isomer shifts was ignored and the spectra were all fit with a single linewidth for all components. The linewidth is larger that the ~0.24 mm/s observed in the α-iron foil calibration spectrum. This increase in linewidth probably results from the distribution of the quadrupole interactions and of isomer shifts which is ignored in our fits.

In the fitting model, each of the seven magnetically inequivalent iron sites is characterized by four hyperfine parameters, its isomer shift, quadrupole shift, maximum hyperfine field, and decremental field. Hence, there is a maximum of 28 adjustable hyperfine parameters. However, the isomer shifts of the crystallographically equivalent sites are constrained to be equal, and this constraint reduces the number of parameters to 25. In addition, the seven quadrupole shift values were obtained from fits with seven broadened sextets and consequently constrained to these values in the binomial distribution fits. Hence, the number of hyperfine parameters adjusted in these fits is 18. In addition, a linewidth and a total absorption area were fit, bringing the total number of adjustable parameters to 20. A doublet with an area of ~2%–5% of the total absorption area was included in all the Mössbauer spectral fits. This doublet has a quadrupole splitting of ~1.0 mm/s, which is independent of temperature and an isomer shift of ~0.08 mm/s at 85 K and of ~0.10 mm/s at 295 K.

The hyperfine parameters resulting from the distribution fits of the Mössbauer effect spectra of $Ce_2Fe_{17-x}Si_x$ measured at 85, 155, 225, and 295 K are given in Table III. The binomial distribution fits of the spectra measured at 85 and 295 K are shown in Figures 6 and 7. The 85 K weighted average maximum hyperfine field $H_{\max}$, shown in Fig. 8, reaches a maximum of ~250 kOe for $Ce_2Fe_{16}Si$ and decreases by ~5 kOe per substituted silicon for higher values of x, a decrease which is due to the dilution of the magnetic moment by silicon. The increase in $H_{\max}$ of ~17 kOe between $Ce_2Fe_{16}Si$ and $Ce_2Fe_{15}Si_2$ at 295 K results because these measurements are just below the Curie temperature which is increasing with x. $Ce_2Fe_{16.77}Si_{0.23}$ is paramagnetic at 225 and 295 K and $H_{\max}$ is zero. Hence, these points are omitted from Fig. 8. As is usually observed in R_2Fe_{17} compounds,[15] the maximum hyperfine fields in $Ce_2Fe_{17-x}Si_x$ follow the order $H_{\max}(6c)>H_{\max}(18f)\gtrsim H_{\max}(9d)>H_{\max}(18h)$, the order of decreasing number of iron near neighbors and the order of the neutron-diffraction-determined magnetic moments observed in $Ce_2Fe_{13.8}Si_{3.2}$, see Table II.

The presence of silicon in the $Ce_2Fe_{17-x}Si_x$ lattice reduces the internal hyperfine field at each site at all temperatures. The weighted average $H_{\max}$ at 85 K for $Ce_2Fe_{17-x}Si_x$ is lower than for $R_2Fe_{17-x}M_x$, where R is Tb or Nd and M is Al or Ga.[2,25,26] Similarly, the average saturation magnetic moment of $\sim 1.8\mu_B$, see Table I, in $Ce_2Fe_{17-x}Si_x$, is lower than the average magnetic moments measured[25,26] by neutron diffraction at 10 K in $Nd_2Fe_{17-x}Al_x$ and $Tb_2Fe_{17-x}Al_x$. The smaller fields observed in $Ce_2Fe_{17-x}Si_x$ may be related to the virtually zero magnetic moment[22] carried by cerium as compared to the rather large magnetic moments[25,26] carried by neodymium and terbium. The weighted average $H_{\max}$ decreases slightly with increasing silicon content. This decrease is expected because of the overall increase in the dilution of magnetic moments due to the substitution of iron by diamagnetic silicon. However, such a small decrease, ~2.5 kOe per silicon, indicates that the hyperfine field, and hence the magnetic moment, at an iron site surrounded only by iron is virtually unaffected by the presence of silicon in subsequent shells of neighbors. In other words, there is no long range influence on the magnetic interactions by the silicon which acts as magnetic holes, as has already been observed[27,28] in FeSi alloys.

The weighted average ΔH at several temperatures is shown in Fig. 9 as a function of silicon content. ΔH remains virtually constant with increasing x between values of 14 and 10 kOe at 85 and 295 K. A similar behavior has been observed[12] for $Nd_2Fe_{17-x}Si_x$ and indicates that the iron moments at different sites remain essentially unperturbed by second-neighbor silicon atoms, suggesting the absence of a cooperative silicon effect via the conduction band, and hence, the absence of transferred hyperfine field via the $4s$ conduction electrons. The constant value of ΔH with x for the $Ce_2Fe_{17-x}Si_x$ solid solutions is in contrast with the variation in ΔH observed in the FeSi alloys,[29,30] a variation which results from the oscillatory behavior of the exchange interaction with the interatomic distance.

In all the Mössbauer spectral fits the isomer shifts of the crystallographically equivalent iron sites in $Ce_2Fe_{17-x}Si_x$ have been constrained to be equal. As shown in Fig. 10, the weighted average isomer shift increases by 0.012 and 0.045 mm/s per substituted silicon at 85 and 295 K, respectively. Approximately the same value and variation of the isomer shift was reported for the FeSi binary alloy[29,30] and for the $Nd_2Fe_{17-x}Si_x$ solid solutions.[12] Compared to $Ce_2Fe_{17-x}Si_x$, higher isomer shifts have been observed[6] in $Nd_2Fe_{14-x}Si_xB$ and $Y_2Fe_{14-x}Si_xB$, resulting from the additional coordination of boron. The increase in $Ce_2Fe_{17-x}Si_x$ occurs in spite of the decrease in unit-cell volume with silicon content. The temperature dependence of the isomer shifts leads to effective masses[31] m_{eff} for the $Ce_2Fe_{17-x}Si_x$ solid solutions in the range of 80–90 g/mol. These values are higher than the values found[32–34] for related R_2Fe_{17} compounds and indicate the importance of covalency in these compounds.

Attempts have been made to explain the increase in the observed isomer shift in the binary FeAl and FeSi alloys by assuming a screening of the majority d electrons[35] and by Friedel oscillations.[36] According to the model proposed by Ingalls, van der Woude, and Sawatzky[37] the change in the charge density at the nucleus $\Delta\rho(0)$ varies with Δn_s and Δn_d, the changes in the number of s and d electrons, respec-

TABLE III. The Mössbauer spectral hyperfine parameters for $Ce_2Fe_{17-x}Si_x$.

x	T, K		$6c$	$9d_6$	$9d_3$	$18f_{12}$	$18f_6$	$18h_{12}$	$18h_6$	Avg.	Γ, mm/s
0.23	85	H_{max}, kOe	304	254	238	238	255	232	227	240	
	155		232	187	180	183	202	180	171	184	
	85	ΔH, kOe	9	12	6	15	10	15	7	11	
	155		17	15	5	14	15	18	8	14	
	85	δ^a, mm/s	0.20	−0.16	−0.16	0.06	0.06	0.01	0.01	0.02	0.34
	155		0.12	−0.14	−0.14	0.03	0.03	−0.10	−0.10	−0.03	0.44
	225		−0.10	−0.10		−0.11		−0.10		−0.10	0.33
	295		−0.15	−0.15		−0.15		−0.14		−0.15	0.33
	225	ΔE_Q, mm/s	0.71	0.70		0.70		0.44		0.60	
	295		0.70	0.70		0.70		0.44		0.60	
1.02	85	H_{max}, kOe	315	264	241	242	269	236	234	249	
	155		277	241	217	222	246	214	211	225	
	225		243	207	188	193	210	184	176	194	
	295		180	141	140	138	155	122	106	136	
	85	ΔH, kOe	17	16	5	14	15	18	8	14	
	155		15	15	5	14	12	17	8	13	
	225		15	14	4	14	12	16	7	12	
	295		13	11	4	11	10	15	6	11	
	85	δ^a, mm/s	0.20	−0.04	−0.04	0.06	0.06	−0.02	−0.02	0.03	0.35
	155		0.17	−0.08	−0.08	0.04	0.04	−0.06	−0.06	0.00	0.33
	225		0.14	−0.11	−0.11	−0.03	−0.03	−0.10	−0.10	−0.02	0.38
	295		−0.03	−0.16	−0.16	−0.10	−0.10	−0.12	−0.12	−0.10	0.44
1.98	85	H_{max}, kOe	308	266	248	243	263	230	217	245	
	155		291	246	231	231	251	220	216	233	
	225		264	230	209	212	231	203	201	214	
	295		231	184	185	185	208	183	172	187	
	85	ΔH, kOe	17	15	4	12	16	18	8	13	
	155		15	15	6	13	12	17	8	13	
	225		15	14	4	14	12	16	7	12	
	295		13	11	4	11	10	15	6	10	
	85	δ^a, mm/s	0.20	−0.04	−0.04	0.07	0.07	0.01	0.01	0.04	0.34
	155		0.19	−0.06	−0.06	0.05	0.05	0.00	0.00	0.03	0.32
	225		0.15	−0.12	−0.12	0.04	0.04	−0.70	−0.70	−0.01	0.34
	295		0.07	−0.16	−0.16	−0.02	−0.02	−0.08	−0.08	−0.05	0.35
3.20	85	H_{max}, kOe	307	256	246	239	261	227	209	236	
	155		289	236	227	226	251	216	203	223	
	225		271	228	209	217	232	202	192	211	
	295		237	193	198	194	216	188	172	190	
	85	ΔH, kOe	17	16	5	12	16	18	8	13	
	155		15	15	5	12	13	17	8	12	
	225		15	14	4	14	12	16	7	12	
	295		13	11	4	11	10	15	6	10	
	85	δ^a, mm/s	0.23	−0.06	−0.06	0.11	0.11	0.05	0.05	0.07	0.33
	155		0.20	−0.05	−0.05	0.05	0.05	0.04	0.04	0.04	0.33
	225		0.19	−0.09	−0.09	0.04	0.04	0.02	0.02	0.02	0.37
	295		0.19	−0.17	−0.17	−0.03	−0.03	−0.05	−0.05	−0.04	0.38

[a]Relative to room-temperature natural abundance α-iron foil.

tively. The increase with x of the Curie temperature of $Ce_2Fe_{17-x}Si_x$, and of the exchange coupling constant J_{FeFe}, see Table I, may result from an electron transfer from silicon to the $3d$ band of iron as was proposed[38] for $Dy_2Fe_{17-x}Al_x$ and $Y_2Fe_{17-x}Al_x$. However, such a charge transfer would increase the isomer shift more substantially than is observed. Hence, we conclude that the number of electrons in the $3d$ band of $Ce_2Fe_{17-x}Si_x$ is essentially independent of x and that $\Delta\rho(0)$ depends only on Δn_s. This conclusion is also supported[30] by the analysis in terms of Δn_s of the change in isomer shift observed in a large number of iron alloys diluted with a variety of elements across the periodic table. The change in the distribution of charge in the s band Δn_s can arise from the hybridization between the iron $4s$ conduction

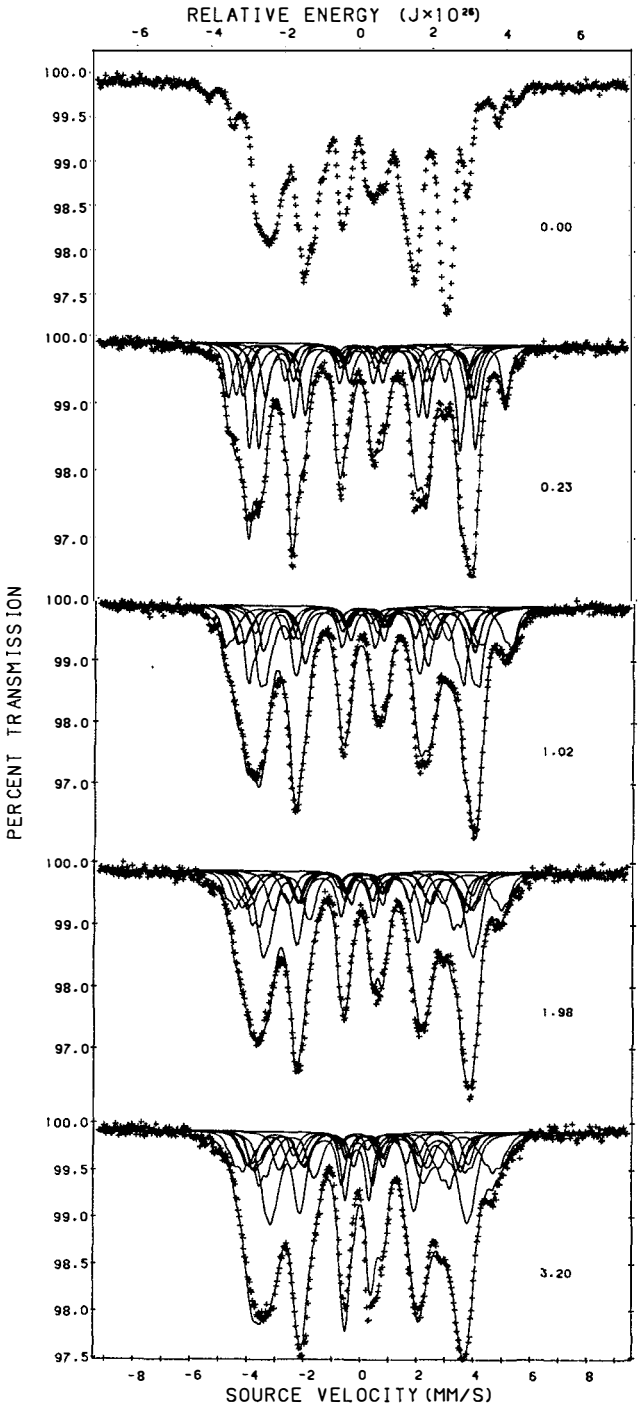

FIG. 6. The 85 K Mössbauer spectra of $Ce_2Fe_{17-x}Si_x$, as a function of the indicated silicon content x, fit with a binomial distribution of near-neighbor environments.

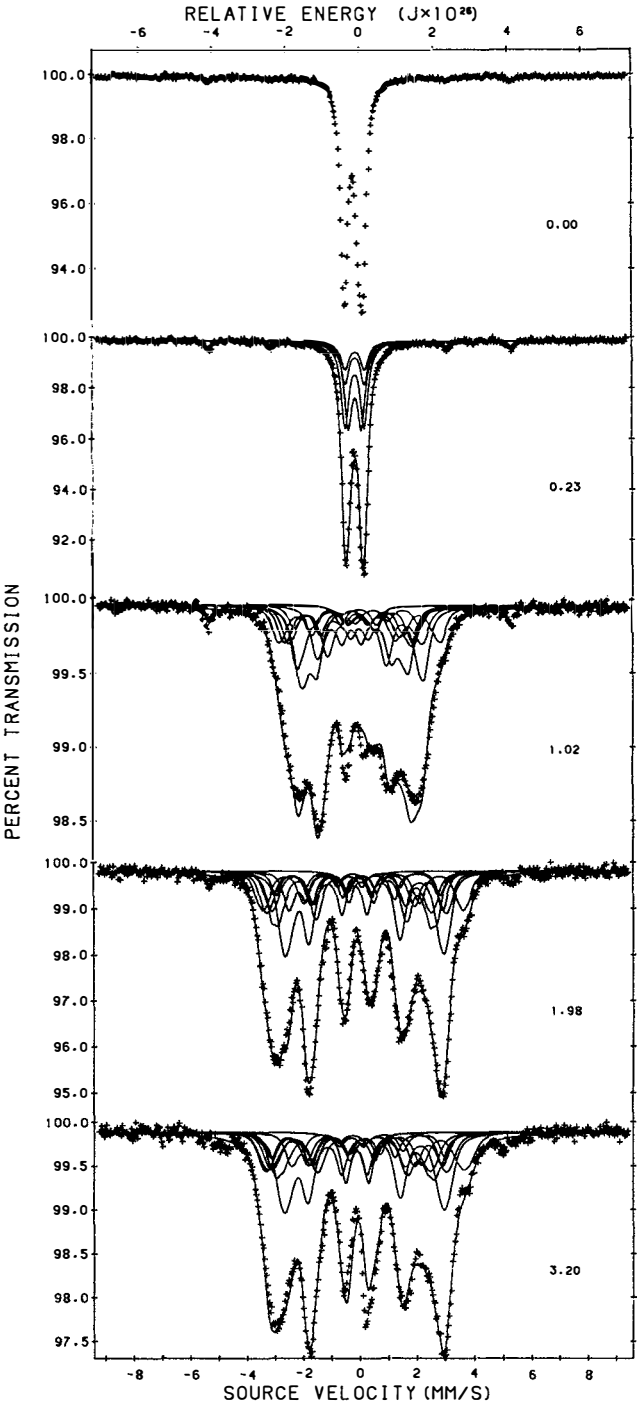

FIG. 7. The 295 K Mössbauer spectra of $Ce_2Fe_{17-x}Si_x$, as a function of the indicated silicon content x, fit with a binomial distribution of near-neighbor environments.

and near-neighbor silicon $2p$ bands, as was already proposed[39] to occur between iron and nitrogen near-neighbor atoms in iron–nitrogen compounds. The reduction in the $6c-18h$, $9d-18h$, $18f-18h$, and $18h-18h$ bond lengths, as shown in Fig. 11, leads to a stronger interband mixing of the iron $4s$ and silicon $2p$ bands. The interband mixing produces the charge redistribution of the $4s$ conduction electrons, such that the isomer shift increases. Because weighted average $H_{\max}$ and ΔH remain virtually unchanged with the addition of silicon, as discussed above, we conclude that this interband mixing does not alter the spin distribution of the $4s$ conduction electrons.

IV. DISCUSSION

The results obtained in the course of this investigation are interesting because they may contribute to elucidating the

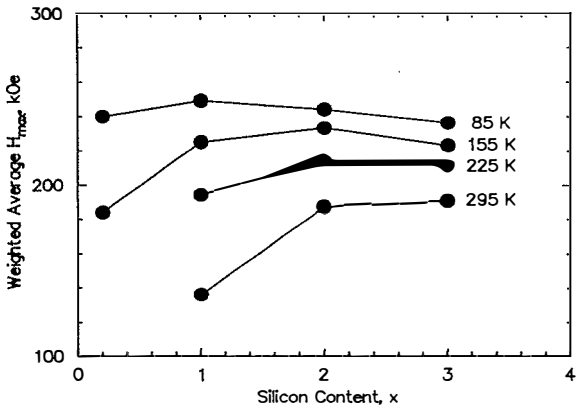

FIG. 8. The weighted average maximum hyperfine field H_{max} measured at several temperatures.

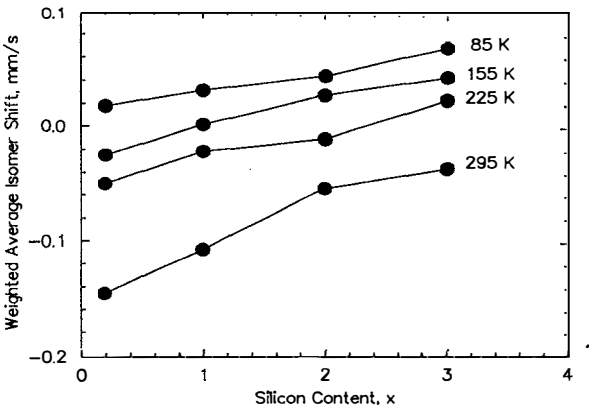

FIG. 10. The weighted average isomer shift from the distribution fits.

origin of the Curie temperature enhancement observed in several series of rare-earth compounds of the type $R_2Fe_{17-x}M_x$, where M is Al, Ga, or Si. The comparatively low Curie temperatures of the R_2Fe_{17} compounds are frequently associated with the presence of the iron $6c-6c$ dumbbell pairs having a rather short iron–iron bond length. The corresponding antiferromagnetic interaction between these dumbbell pairs is believed to be responsible for the low Curie temperatures of the R_2Fe_{17} compounds. The neutron-diffraction results obtained in the course of this investigation show that silicon does not replace iron on the dumbbell sites, indicating that the removal of the iron dumbbell atoms by silicon substitution cannot explain the increase in Curie temperature with increasing silicon content. A similar conclusion was reached earlier from a neutron-diffraction and Mössbauer spectral study[2] of the $Tb_2Fe_{17-x}Ga_x$ solid solutions.

Descriptions of the Curie temperature in terms of distance-dependent exchange coupling,[40] or in terms of spin-fluctuation theory,[13,41] have in common that the Curie temperature depends on the lattice dimensions. In the case of $Tb_2Fe_{17-x}Ga_x$ we found that the Curie temperature enhancement is accompanied by an expansion of the lattice in both the a- and the c-axis lattice directions. In contrast, the results for $Ce_2Fe_{17-x}Si_x$ reveal that the Curie temperature enhancement is accompanied by a contraction of the lattice in the a direction and an expansion of the lattice in the c direction. From these results it may be concluded that changes in the a-axis lattice direction are relatively unimportant for the Curie temperature enhancement in R_2Fe_{17} compounds. Our results also indicate that an overall volume expansion is not responsible for the Curie temperature enhancement, because the unit-cell volume decreases with increasing x in $Ce_2Fe_{17-x}Si_x$.

In order to further assess the possible influence of the changes in bond length on the Curie temperature we have calculated the concentration dependence of the bond lengths

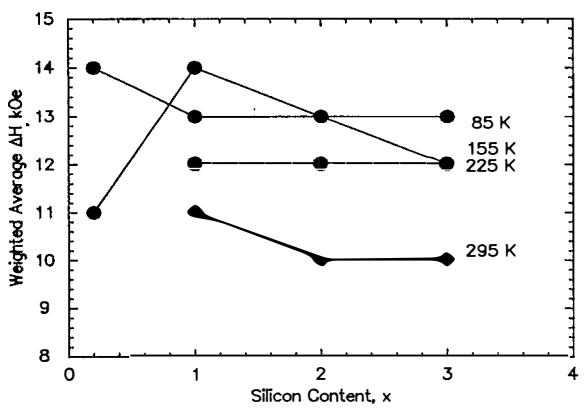

FIG. 9. The weighted average decremental hyperfine field ΔH measured at several temperatures.

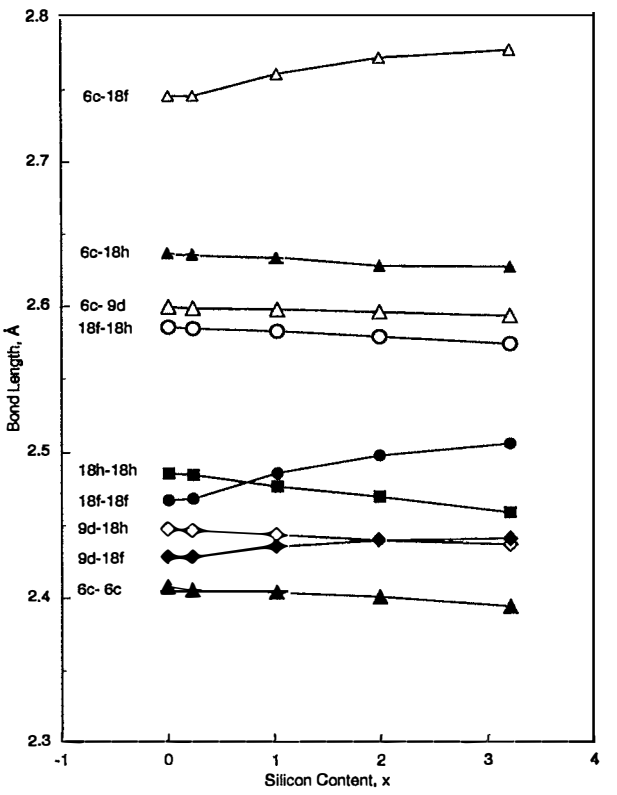

FIG. 11. The concentration dependence of the bond lengths in $Ce_2Fe_{17-x}Si_x$, as derived from the refinement results listed in Table II.

in $Ce_2Fe_{17-x}Si_x$ from the atomic positional parameters listed in Table II. The results of these calculations are shown in Fig. 11 and indicate that silicon substitution into Ce_2Fe_{17} leads to both increases and decreases in the interatomic separations associated with the various atomic sites. Most interesting and surprising is the iron $6c-6c$ dumbbell separation which decreases with x even though the c-axis lattice parameter increases with x. This result again indicates that it is highly unlikely that changes in Curie temperature originate from changes in the $6c-6c$ dumbbell atom separation.

Finally, we wish to note that the decrease in unit-cell volume of $Ce_2Fe_{17-x}Si_x$ with increasing x is realized by a decrease in the a-axis lattice parameter accompanied by an increase in the c-axis lattice parameter. The latter increase is very likely a result of magnetovolume effects that come into play when the Curie temperature is increased from below room temperature, when $x=0.0$ and 0.23, to above room temperature when $x=1$, 2, and 3.

ACKNOWLEDGMENTS

The authors acknowledge, with thanks, NATO for Cooperative Scientific Research Grant No. 92-1160, and the Division of Materials Research of the U.S. National Science Foundation, for Grants No. DMR-9214271 and DMR-9305782. D.P.M. would like to acknowledge the stimulating support of L. J. de Jongh and to thank the Stichting voor Fundamenteel Onderzoek der Materie, which is financially supported by the Nederlandse Organisatie voor Wetenschappelijk Onderzoek.

[1] J. M. D. Coey and H. Sun, J. Magn. Magn. Mater. **87**, L251 (1990); H. Sun. J. M. D. Coey, Y. Otani, and D. P. Hurley, J. Phys. Condens. Matter **2**, 6465 (1990).
[2] Z. Hu, W. B. Yelon, S. Mishra, G. J. Long, O. A. Pringle, D. P. Middleton, K. H. J. Buschow, and F. Grandjean, J. Appl. Phys. **76**, 443 (1994).
[3] D. P. Middleton and K. H. J. Buschow, J. Alloys Comp. **203**, 217 (1994).
[4] A. T. Pedziwiatr and W. E. Wallace, J. Less-Common Met. **126**, 41 (1986).
[5] M. Morariu, M. Rogalski, N. Plugaru, M. Valeanu, and D. P. Lazar, J. Phys. D (to be published).
[6] G. K. Marasinghe, O. A. Pringle, G. J. Long, W. J. James, D. Xie, J. Li, W. B. Yelon, and F. Grandjean, J. Appl. Phys. **74**, 6798 (1993); G. K. Marasinghe, O. A. Pringle, G. J. Long, W. B. Yelon, and F. Grandjean, *ibid.* **76**, 2960 (1994).
[7] R. van Mens, J. Magn. Magn. Mater. **61**, 24 (1993).
[8] E. E. Alp, A. M. Umarji, S. K. Malik, G. K. Shenoy, M. Q. Huang, E. B. Boltich, and W. E. Wallace, J. Magn. Magn. Mater. **86**, 305 (1987).
[9] P. C. M. Gubbens, A. M. van der Kraan, T. H. Jacobs, and K. H. J. Buschow, J. Less-Common Met. **159**, 173 (1990).
[10] C. Lin, Y. X. Sun, Z. X. Liu, H. W. Jiang, G. Jiang, J. L. Yang, B. S. Zhang, and Y. F. Ding, Solid State Commun. **81**, 299 (1992).
[11] D. P. Middleton and K. H. J. Buschow, J. Alloys Comp. **206**, L1 (1994).
[12] G. J. Long, G. K. Marasinghe, S. Mishra, O. A. Pringle, F. Grandjean, K. H. J. Buschow, D. P. Middleton, W. B. Yelon, F. Pourarian, and O. Isnard, Solid State Commun. **88**, 761 (1993).
[13] J. P. Woods, B. M. Patterson, A. S. Fernando, S. S. Jaswal, D. Welipitya, and D. J. Sellmyer, Phys. Rev. B **51**, 1064 (1995).
[14] FULLPROF Rietveld refinement written by J. Rodriguez-Carjaval, Institute Laue Langevin, Grenoble, France.
[15] F. Grandjean and G. J. Long, in *Interstitial Intermetallic Alloys*, edited by F. Grandjean, G. J. Long, and K. H. J. Buschow (Kluwer, Dordrecht, 1995), p. 463.
[16] D. Givord and R. Lemaire, IEEE Trans. Magn. **MAG-10**, 109 (1974).
[17] K. H. J. Buschow and J. S. van Wieringen, Phys. Status Solidi **42**, 231 (1970).
[18] O. I. Bodek and E. I. Gladyshevskii, *Handbook of Ternary Systems Containing Rare-Earth Metals* (L'vov State University Press, Moscow, 1985), p. 215.
[19] M. Valeanu, N. Plugaru, and E. Burzo, Solid State Commun. **89**, 519 (1994).
[20] R. Coehoorn, Phys. Rev. B **39**, 13 072 (1989).
[21] T. W. Capehart, R. K. Mishra, G. P. Meisner, C. D. Fuerst, and J. F. Herbst, Appl. Phys. Lett. **63**, 362 (1993).
[22] O. Isnard, S. Miraglia, D. Fruchart, C. Giorgetti, S. Pizzini, E. Dartyge, G. Krill, and J. P. Kappler, Phys. Rev. B **49**, 15 692 (1994).
[23] K. H. J. Buschow, Rev. Prog. Phys. **40**, 1179 (1977).
[24] M. Kawakami, T. Hihara, Y. Koi, and T. Wakiyama, J. Phys. Soc. Jpn. **33**, 1591 (1972).
[25] G. J. Long, G. K. Marasinghe, S. Mishra, O. A. Pringle, Z. Hu, W. B. Yelon, D. P. Middleton, K. H. J. Buschow, and F. Grandjean, J. Appl. Phys. **76**, 5383 (1994).
[26] G. K. Marasinghe, S. Mishra, O. A. Pringle, G. J. Long, Z. Hu, W. B. Yelon, F. Grandjean, D. P. Middleton, and K. H. J. Buschow, J. Appl. Phys. **76**, 6731 (1994).
[27] M. B. Stearns, Phys. Rev. B **9**, 3326 (1972).
[28] M. B. Stearns, Phys. Rev. B **13**, 1183 (1976).
[29] M. B. Stearns, Phys. Rev. **147**, 439 (1966).
[30] H. Akai, S. Blügel, R. Zeller, and P. H. Dederichs, J. Magn. Magn. Mater. **54**, 1101 (1986).
[31] R. H. Herber, in *Chemical Mössbauer Spectroscopy*, edited by R. H. Herber (Plenum, New York, 1984), p. 199.
[32] G. J. Long, O. A. Pringle, F. Grandjean, and K. H. J. Buschow, J. Appl. Phys. **72**, 4845 (1992).
[33] G. J. Long, O. A. Pringle, F. Grandjean, W. B. Yelon, and K. H. J. Buschow, J. Appl. Phys. **74**, 504 (1993).
[34] G. J. Long, O. A. Pringle, F. Grandjean, T. H. Jacobs, and K. H. J. Buschow, J. Appl. Phys. **75**, 2598 (1994).
[35] G. Grüner, I. Vincze, and L. Cser, Solid State Commun. **10**, 347 (1972).
[36] I. Vincze and A. Campbell, J. Phys. F **3**, 647 (1973).
[37] R. Ingalls, F. van der Woude, and G. A. Sawatzky, in *Mössbauer Isomer Shifts*, edited by G. K. Shenoy and F. E. Wagner (North-Holland, Amsterdam, 1978), p. 361.
[38] D. Plusa, R. Pfranger, and B. Wyslocki, J. Less-Common Met. **99**, 87 (1984).
[39] W. Zhou, L. J. Qu, Q. M. Zhang, and D. S. Wang, Phys. Rev. B **40**, 6393 (1989).
[40] S. A. Nikitin, A. M. Tishin, M. D. Kuzmin, and Yu. I. Spichkin, Phys. Lett. A **153**, 155 (1991).
[41] Q. N. Qi, R. Skomski, and J. M. D. Coey, J. Phys. Condens. Matter **6**, 32 (1994).